01 Jan 2005

Spin-System Radio-Frequency Superradiation: A Phenomenological Study and Comparison with Numeric Simulations

Carrie L. Davis

Victor K. Henner

Aleksandr V. Chernatynskiy
Missouri University of Science and Technology, aleksandrc@mst.edu

Ilia V. Kaganov

Recommended Citation

C. L. Davis et al., "Spin-System Radio-Frequency Superradiation: A Phenomenological Study and Comparison with Numeric Simulations," *Physical review B: Condensed matter and materials physics*, vol. 72, no. 5, American Physical Society (APS), Jan 2005.
The definitive version is available at https://doi.org/10.1103/PhysRevB.72.054406

Spin-system radio-frequency superradiation: A phenomenological study and comparison with numeric simulations

C. L. Davis, V. K. Henner, A. V. Tchernatinsky, and I. V. Kaganov
Department of Physics, University of Louisville, Louisville, Kentucky 40292, USA
and Department of Theoretical Physics, Perm State University, Perm, 614600, Russia
(Received 27 May 2003; revised manuscript received 22 February 2005; published 2 August 2005)

We discuss the coherent behavior of a polarized, nuclear or electron, spin system for which the magnetic dipole radiation emitted in the radio-frequency region, has approximately quadratic dependence on the number of spins. An effective method of describing these phenomena is provided by computer simulation of a microscopic model of the spin system. Important aspects of this numeric simulation are described, together with a comparison with the theoretical predictions. The behavior of the transverse component of the magnetic moment, $M^+(t)$, in super-radiant conditions is studied. In addition, the role of dipole-dipole interactions in superradiation phenomena is investigated in detail. It is shown that some important features of super-radiation cannot be described with the Bloch equations.

DOI: 10.1103/PhysRevB.72.054406 PACS number(s): 76.60.−k, 76.30.−v

I. INTRODUCTION

One of the manifestations of the phenomenon of superradiation (SR) is that the radiation intensity can be N times the incoherent radiation from a system of N radiators. The properties of such coherent effects in optics, for example, super-fluorescence, super-luminescence, collective induction and photon echo, have been extensively studied.[1] An effect similar to optical super-fluorescence, but in the radio-frequency region, is much less well known. It is this SR phenomenon which is the topic of this study.

Although this phenomenon is very similar to optical super-fluorescence, the physics governing SR in nuclear or electron spin systems is very different and is more naturally described using traditional magnetic resonance (MR) methods. Magnetic resonance methods are well understood (for example Abragam and Goldman's book[2]) and were first applied to this SR phenomenon in Refs. 3 and 4. From a physical standpoint, the main difference between SR from nuclear or electron spin systems and the SR in optical case is that the radio-frequency wavelength is much longer than the size of the system so that propagation effects do not play a role. Bloembergen and Pound investigated[5] the collective behavior of a system of nuclear spins under the influence of a resonator feedback field and showed that the relaxation time of nuclear induction can become much shorter than the spin dephasing time. Although they considered collective induction, rather than SR, their results were later used to argue that it might be experimentally possible to obtain a measurable SR signal using the resonator feedback field. A SR signal was indeed successfully observed experimentally for several spin systems by, for example, Bosiger *et al.*[6] and Kiselev *et al.*[7] Some recent studies of SR are described in Ref. 8.

In experiments measuring SR from nuclear spins,[7] the super-radiance from protons in propandiol ($C_3H_8O_2$) was detected. The sample was kept at a temperature of about 0.1 K in a magnetic field, $H_0 \approx 2.6 \times 10^4$ G. The proton spins were dynamically polarized by imposing a high-frequency magnetic field on the wing of the EPR resonance line of low concentration Cr^{5+} ion impurities in the propandiol. Due to energy exchange with the electron spin system of paramagnetic ions, the proton spin system dynamically cools, thus achieving a large polarization. In these experiments, after cooling, the material is frozen at a temperature of about 5×10^{-2} K, which corresponds to a proton polarization of about 90%. At this temperature the spin-lattice interaction is very weak, the relaxation is very slow and the polarization lifetime is measured in tens of hours. Prepared in such a way, the polarized sample (with a volume of about 0.5 cm^3) is placed in a passive resonant electric coil and a strong permanent magnetic field, H_0, directed antiparallel to the total magnetic moment of the sample. In this way, the spin system is prepared in an inverted, strongly nonequilibrium state. SR is observed when the proton Larmor frequency, ω_0, is equal to the resonant frequency of the passive resonant coil, $\omega_c \approx 10^8$ Hz (radio-frequency region). For large polarizations a sharp SR peak is observed due to feedback from the passive resonant coil, while the nuclear spins coherently flip to the equilibrium state.

References 3, 4, and 9 describe numeric simulations based on a microscopic description of this type of SR from a homogeneous spin system. One of the results of these numerical calculations is that if the SR delay and pulse times are short enough, dipole-dipole interactions play a very weak role in observable phenomena. If dipole-dipole interactions are ignored, the behavior of the system is governed by the interaction of the spins with the external magnetic field and the external circuit. The precession of the spins about the external magnetic field takes place on a time scale dependent on the magnitude of the field. Whereas the interaction of the spins with the external circuit takes place on a time scale longer or shorter than the first scale, depending on the initial parameters.

Section II of this article briefly describes the microscopic model of a system of spins which forms the basis of our numeric simulation and phenomenological approach. In Sec. III, dipole-dipole interactions are incorporated into the single particle model by including transverse Bloch damping terms

into the equation of motion of the system. Methods of achieving a desired initial distribution of spins, and the use of parallel computing architecture in the numeric simulation are described in Sec. IV. In Sec. V theoretical predictions are compared to results of the numeric simulation. Particular attention is paid to the behavior of the transverse component of the magnetic moment, since this is a critical quantity in magnetic resonance experiments.

II. MICROSCOPIC SPIN MODEL

Consider a system of N spins whose sites are enumerated by the index $i=1,2,\ldots,N$. The spin operator $\mathbf{s}_i$ corresponds to the effective spin $s=1/2$ of the paramagnetic ions (or nuclei) at the nodes of a regular rigid simple-cubic lattice. The dipole interaction of spins has the form

$$\mathcal{H}_{ij}=\frac{\boldsymbol{\mu}_i\boldsymbol{\mu}_j}{r_{ij}^3}-\frac{3(\boldsymbol{\mu}_i\cdot\mathbf{r}_{ij})(\boldsymbol{\mu}_j\cdot\mathbf{r}_{ij})}{r_{ij}^5}, \tag{1}$$

where $\mathbf{r}_{ij}=\mathbf{r}_i-\mathbf{r}_j$, $r_{ij}=|\mathbf{r}_{ij}|$ and the magnetic moment $\boldsymbol{\mu}_i=\mu\mathbf{s}_i$, where $\mu=\gamma\hbar$ and γ is the gyromagnetic ratio ($\gamma>0$ for protons, $\gamma<0$ for electrons).

The system is under the influence of a constant external magnetic field $\mathbf{H}_0$. Including a passive electric resonant circuit, tuned to the Zeeman frequency, $\omega_0=\gamma H_0$, the system also feels an additional magnetic field $\mathbf{H}_{\rm res}$, induced by the rotating spins of the system. The coupling of the spin system with the external circuit causes a rapid coherent relaxation of the nonequilibrium state that produces a SR pulse. The *emf* and magnetic field induced in the circuit are classical macroscopic quantities due to the collective action of all the spins in the system. The *emf* is given by

$$U_{\rm ind}=-\frac{1}{c}\frac{d\Phi}{dt}=-\frac{1}{c}\frac{d}{dt}\left(\frac{4\pi\eta n\mu}{l}\sum_i^N\langle\mathbf{s}_i\rangle\cdot\mathbf{e}_c\right)$$

$$=-\frac{4\pi\eta An\mu}{cV}\frac{d}{dt}\sum_i\langle\mathbf{s}_i\rangle\cdot\mathbf{e}_c, \tag{2}$$

where $\langle\cdots\rangle$ represents the statistical average, corresponding to the mean polarization of the spin system at a particular temperature;[10] n is the number of turns in the circuit with cross section A, volume V, and length l. $\mathbf{e}_c$ is a unit vector in the direction of the axis of the circuit and η is the filling factor of the coil ($\eta<1$). The magnetic field induced in the circuit is then given by

$$H_{\rm res}=\frac{4\pi}{c}\frac{n}{l}j=\frac{4\pi}{c}\frac{n}{l}\frac{U_{\rm ind}}{R}=-\left(\frac{4\pi}{c}\right)^2\frac{n^2\eta\mu}{l^2R}\frac{d}{dt}\sum_i\langle\mathbf{s}_i\rangle\cdot\mathbf{e}_c, \tag{3}$$

where R is the resistance and j the current in the circuit. The inductance and the quality factor of the circuit are, respectively, $L=4\pi n^2A/lc^2$ and $Q=\omega L/R$. We imply that the circuit frequency $\omega=(LC)^{-1/2}$ is in resonance with the Zeeman frequency, $\omega=\omega_0$. With the coil axis orthogonal to the constant field $\mathbf{H}_0$ and taken along $\mathbf{e}_x$, the induced magnetic field can be written

$$\mathbf{H}_{\rm res}=H_{\rm res}\mathbf{e}_x=-\frac{2g}{\gamma}\mathbf{e}_x\frac{d}{dt}\sum_i\langle s_i^x\rangle, \tag{4}$$

where

$$g=\frac{1}{2}\left(\frac{4\pi}{c}\right)^2\left(\frac{n}{l}\right)^2\frac{\eta\mu\gamma}{R}. \tag{5}$$

g is a measure of the coupling between the spin system and the resonant circuit. With $n/l=10^4\ \mathrm{m}^{-1}$, $R=10\ \Omega$ (values similar to those of Kiselev[7]), g is approximately 10^{-20} for electrons and 10^{-25} for protons. As will be shown later, the product gN, where N is the number of spins in the system, is critical in determining the behavior of the system. For a sample of containing 10^{22} spins, gN has the value 10^{-3} for protons and 10^2 for electrons.

Ignoring inhomogeneous widening, the total Hamiltonian of the system has the form

$$\hat{\mathcal{H}}=-\mu H_0\sum_i s_i^z-\frac{1}{2}\mu H_{\rm res}\sum_i(s_i^+ + s_i^-)+\hat{\mathcal{H}}_d, \tag{6}$$

where the dipole-dipole interaction Hamiltonian is given by

$$\hat{\mathcal{H}}_d=\frac{1}{2}\sum_{i\neq j}\left\{a_{ij}\left(s_i^zs_j^z-\frac{1}{2}s_i^+s_j^-\right)+2c_{ij}s_i^+s_j^z\right.$$

$$\left.+2c_{ij}^*s_i^zs_j^-+e_{ij}s_i^+s_j^++e_{ij}^*s_i^-s_j^-\right\}, \tag{7}$$

$s^\pm=s_x\pm is_y$, and the coefficients a_{ij}, c_{ij}, e_{ij} are

$$a_{ij}=\frac{\gamma^2\hbar^2}{r_{ij}^3}(1-3\cos^2\theta_{ij}),$$

$$c_{ij}=-\frac{3\gamma^2\hbar^2}{4r_{ij}^3}\sin 2\theta_{ij}\exp(-i\phi_{ij}),$$

$$e_{ij}=-\frac{3\gamma^2\hbar^2}{4r_{ij}^3}\sin^2\theta_{ij}\exp(-2i\phi_{ij}). \tag{8}$$

In MR applications solutions are typically obtained via perturbation theory based on the (small) quantity $|H_{\rm loc}/H_0|$, where $H_{\rm loc}$ represents the local magnetic fields.[2] However, coherent effects are described by nonlinear equations for which the perturbation method is not applicable. In this case, the equations of motion must be solved using the total Hamiltonian (6), rather than only the secular terms (those including a_{ij}) of dipole-dipole interactions.

Using the Heisenberg equations of motion for the spin operators, $i\hbar(d/dt)s_i^\alpha=[s_i^\alpha,\hat{\mathcal{H}}]$, performing commutations and replacing spin operators with index j with their classical averages, we obtain

$$i\frac{ds_i^z}{dt}=-\frac{g}{2}(s_i^- - s_i^+)\frac{d}{dt}\left\langle\sum_j(s_j^- + s_j^+)\right\rangle+\frac{1}{\hbar}\sum_{j(\neq i)}\left\{\frac{a_{ij}}{4}(s_i^-\langle s_j^+\rangle\right.$$

$$\left.-s_i^+\langle s_j^-\rangle)+(c_{ij}s_i^+-c_{ij}^*s_i^-)\langle s_j^z\rangle+e_{ij}s_i^+\langle s_j^+\rangle-e_{ij}^*s_i^-\langle s_j^-\rangle\right\}, \tag{9}$$

$$i\frac{ds_i^-}{dt} = -\omega_0 s_i^- - g s_i^z \frac{d}{dt}\left\langle \sum_j (s_j^- + s_j^+)\right\rangle + \frac{1}{\hbar}\sum_{j(\neq i)}\left\{\frac{a_{ij}}{2}(s_i^z\langle s_j^-\rangle + 2s_i^-\langle s_j^z\rangle) + c_{ij}(s_i^-\langle s_j^+\rangle - 2s_i^z\langle s_j^z\rangle) + c_{ij}^* s_i^-\langle s_j^-\rangle - 2e_{ij}s_i^z\langle s_j^+\rangle\right\} \quad (10)$$

and the conjugate of Eq. (10). These equations describe the evolution of spin $\mathbf{s}_i$ in the mean field of the other spins, $\mathbf{s}_j$. They can also be obtained from Eq. (7) replacing a product of two operators, $AB \Rightarrow \langle A\rangle B + A\langle B\rangle - \langle A\rangle\langle B\rangle$, equivalent to the mean-field approximation.

III. THE ROLE OF DIPOLE-DIPOLE INTERACTIONS

The realization of equilibrium of a system of spins can be conveniently described in two distinct stages. First, the Zeeman (in the field H_0) and dipole-dipole subsystems form, each with a characteristic, distinct, temperature. In the second stage these two subsystems exchange energy finally reaching thermodynamic equilibrium with a common spin temperature. This stage is described by Provotorov's equations;[11] the characteristic time for this evolution being approximately the dipole-dipole interaction time, T_d. Clearly, dipole-dipole interactions play a central role in this process. However, for times much shorter than T_d, it is well known[2] that dipole-dipole interactions play a very weak role in observable macroscopic magnetic resonance phenomena such as the time evolution of the total magnetization of a sample. Thus, if SR delay and pulse times are much shorter than T_d, dipole-dipole interactions may be neglected in describing SR which results in a rapid inversion of the total magnetization.

Solving Eqs. (9) and (10) by means of numeric simulation, it can also be shown that neglecting the dipole-dipole interaction terms gives practically the same results for macroscopic quantities such as the total magnetization and the intensity of magneto-dipole radiation as solving the equations directly. In contrast, at longer time scales, dipole-dipole interactions, in particular the nonsecular terms, play a critical role in establishing the equilibrium of such a system.

Regarding the role of dipole-dipole interactions, it is important to note that we are not considering the situation where the total polarization vector is initially in exactly the same direction as $\mathbf{H}_0$. In these cases dipole-dipole interactions can play an important role in the evolution of the polarization vector at the very beginning of the process.[8] To describe the process in simple terms, the evolution of the angle θ, between the macroscopic magnetization $\mathbf{M}$ and $\mathbf{H}_0$, can be written[12]

$$\tan\frac{\theta}{2} = \tan\frac{\theta(0)}{2}e^{-t'/2},$$

where $t' = \omega_0 t/\Omega$ ($\Omega \sim 1/gN$, see below). If the magnetization vector initially makes a small angle $\pi - \theta(0)$ with $\mathbf{H}_0$ (where $\theta = \pi$ corresponds to the unstable state), then

$$\tan\frac{\pi-\theta}{2} \approx \frac{1}{2}(\pi - \theta(0))e^{t'/2}$$

and the time of deviation from the initial direction rises logarithmically as $\ln(\pi - \theta(0))$ as $\pi - \theta(0)$ decreases. For $(\pi - \theta(0)) \approx 0.1^0$, the time to reach $\theta = \pi/2$ is given by $t' \approx 20$ (in units of the characteristic SR time $T_c \sim \Omega/\omega_0$). In this time period, transverse relaxation weakens the SR pulse making it more difficult to observe.

However, in a typical MR experiment, such as that of Kiselev,[7] the directional accuracy of the magnetization vector is at best several degrees, meaning that there will always be a significant initial deviation from the direction $\mathbf{H}_0$. Therefore, in these circumstances, if the SR delay and pulse times are much shorter than the characteristic dipole-dipole interaction time, we may safely neglect dipole-dipole interactions when describing the time evolution of the SR process. However, it should be noted that even in this case the behavior of the individual spins are not independent; they interact with each other via the induced feedback magnetic field of a resonator.

It is helpful to present a simple analytical discussion when dipole-dipole interactions are neglected. In this case the system of Eqs. (9) and (10) and the conjugate of Eq. (10) become

$$i\frac{d}{dt}s_i^+ = \omega_0 s_i^+ + g s_i^z \sum_j \frac{d}{dt}\langle s_j^- + s_j^+\rangle,$$

$$i\frac{d}{dt}s_i^- = -\omega_0 s_i^- - g s_i^z \sum_j \frac{d}{dt}\langle s_j^- + s_j^+\rangle,$$

$$i\frac{d}{dt}s_i^z = -\frac{1}{2}g(s_i^- - s_i^+)\sum_j \frac{d}{dt}\langle s_j^- + s_j^+\rangle. \quad (11)$$

Performing statistical averaging and summing over all spins in the system, using the notation $S^+ = (1/N)\Sigma_i\langle s_i^+\rangle$, $S^- = (1/N)\Sigma_i\langle s_i^-\rangle$, $S^z = (1/N)\Sigma_i\langle s_i^z\rangle$, the above system of equations can be solved algebraically for the time derivatives giving,

$$i\frac{d}{dt}S^+ = S^+ - \frac{1}{i}gNS^z(S^- - S^+),$$

$$-i\frac{d}{dt}S^- = S^- + \frac{1}{i}gNS^z(S^+ - S^-),$$

$$\frac{d}{dt}S^z = \frac{gN}{2}(S^- + S^+)^2, \quad (12)$$

where the time scale has been renormalized by setting $t = t/\omega_0$.

It is clear from (12) that the behavior of the system is highly dependent on the value of gN. When $gN \ll 1$ it is dominated by the interaction of the spins with external magnetic field. In contrast, if $gN \gg 1$ the dominant interaction is that of the system with the resonant circuit. Alternatively, if we write the initial magnetization as $M_0 = \mu N\mathcal{L}(\zeta)$, where ζ

$=\mu H_0/k_bT$, T is the temperature of system, k_b is the Boltzmann constant and $\mathcal{L}(\zeta)=\coth\zeta-(1/\zeta)$ is the classical Langevin function, then the feedback field becomes, $H_{\rm res}=-(1/\gamma\Omega M_0)\dot{M}_x$,[12] where Ω is related to gN via $\Omega=1/gN\mathcal{L}$. It is clear that the value of Ω determines the characteristic of the motion. For $\Omega\ll 1$, the tuned coil scenario is forbidden, the motion being aperiodic rather than oscillatory. The characteristic scale of the variation of M_x with respect to t' is found to be of order $\Omega/\gamma H_0$ and the ratio of the energy of interaction of $\mathbf{M}$ with the fields H_0 and $H_{\rm res}$ is $H_0/H_{\rm res}\sim\Omega^2\sim 1/N^2$. On the other hand, if $\Omega\gg 1$, the motion is periodic with frequency $\omega_0=\gamma H_0$, the characteristic scale of the variation of M_x with respect to t' is of order $1/\gamma H_0$ and $H_0/H_{\rm res}\sim\Omega\sim 1/N$. The set of parameters, $R=3$ ohm, $w=5$ cm^{-1}, $N\approx 5\times 10^{23}$, $H_0=0.25\times 10^5$ G and $T=0.3$ K, as used in the NMR experiment of Kiselev *et al.*,[7] gives $\Omega\sim 6000$, corresponding to $gN\ll 1$. Thus, the condition $gN\ll 1$ can be satisfied for some systems of proton spins or a relatively small system of paramagnetic spins.

The method of multitime scales provides a standardized approach to deal with this type of system. It allows the consideration of slow motion in any order through a series expansion in powers of a small parameter. In this case the parameter is the ratio of the characteristic times of slow motion (relaxation with times T_c and T_d) and fast motion (rotation time about the field H_0). Expanding S^+, S^-, S^z and the operator of the derivative d/dt in powers of gN, we obtain

$$\frac{d}{dt}=\frac{d}{dt_0}+gN\frac{d}{dt_1}+\cdots,\quad S^+=S_0^+ + gNS_1^+ +\cdots,$$

$$S^-=S_0^- + gNS_1^-\cdots,\quad S^z=S_0^z+gNS_1^z+\cdots. \tag{13}$$

In "zeroth" order, where all terms involving gN can be ignored, Eq. (12) describe the simple rotation of the magnetic moment around the external field, H_0,

$$S_0^+=A\exp(-it_0),\quad S_0^-=B\exp(it_0),\quad S_0^z=C, \tag{14}$$

where A,B,C may be functions of the times $t_1,t_2,\ldots,$ but not t_0 which corresponds to the Zeeman frequency ω_0. Including terms linear in gN, Eqs. (12) may be written,

$$i\frac{d}{dt_0}S_1^+ - S_1^+ = -i\left(\frac{d}{dt_1}A\right)\exp(-it_0)-\frac{1}{i}C(A\exp(-it_0) - B\exp(it_0)),$$

$$-i\frac{d}{dt_0}S_1^- - S_1^- = i\frac{d}{dt_1}B\exp(it_0)+\frac{1}{i}C(B\exp(it_0) - A\exp(-it_0)),$$

$$i\frac{d}{dt_0}S_1^z=\frac{d}{dt_1}C+\frac{1}{2}(B\exp(it_0)-A\exp(-it_0))^2, \tag{15}$$

where S_0^+, S_0^-, and S_0^z have been substituted from Eq. (14). Equations (15) are nonhomogeneous first order differential equations. If such equations include terms with the same exponents as the exponents which are solutions of the homogeneous equations, then the nonhomogeneous solutions are divergent as t_0 becomes large. For physical, nondivergent, solutions we require these terms be zero, leading to the first two of the following equations:

$$\frac{d}{dt_1}A=CA,\quad \frac{d}{dt_1}B=CB,\quad \frac{d}{dt_1}C=-AB. \tag{16}$$

The third of Eqs. (16) is obtained by averaging over t_0, assuming S_i^z is independent of t_0. Making use of the fact that A and B are complex conjugates, $A=x+iy$, $B=x-iy$, and writing $C=z$ we obtain

$$\frac{d}{dt_1}x=xz,\quad \frac{d}{dt_1}y=yz,\quad \frac{d}{dt_1}z=-(x^2+y^2). \tag{17}$$

Solving for z, gives

$$z=c_1\frac{c_2-e^{2c_1t_1}}{c_2+e^{2c_1t_1}}, \tag{18}$$

where c_1 and c_2 are constants, defined by the initial conditions of the system. With $z(0)=z_0$ and $(d/dt_1)z(0)=-(x_0^2+y_0^2)$, where x_0, y_0, z_0 are the initial components of the total magnetic moment, the constants c_1 and c_2 are given by

$$c_1^2=z_0^2+x_0^2+y_0^2,$$

$$c_2=-\frac{(z_0+\sqrt{z_0^2+x_0^2+y_0^2})^2}{x_0^2+y_0^2}. \tag{19}$$

Assuming an initial polarization making a small angle with the z axis, and having x and y components small compared to the z component, the time taken for the polarization of the system to reach zero is given approximately by Eq. (18), when $z(t_1)\approx 0$,

$$t_1=\frac{\ln(-c_2)}{2c_1}. \tag{20}$$

This time is characteristic of the interaction between the spin system and the external coil. Reverting back to conventional units from the dimensionless t_1 we find

$$t=\frac{\ln(-c_2)}{2c_1gN\omega_0}. \tag{21}$$

Using $z_0=0.475$ (this value corresponds to a polarization of 0.95 for spin 1/2), $x_0=y_0=0.01$, $\omega_0=10^8$ Hz and the characteristic value for a nuclear spin system from Sec. II, $gN=10^{-3}$, the time for the polarization to reach zero is about 10^{-4} s.

The intensity of magneto-dipole radiation is given by

$$I=\frac{2}{3c^3}|\ddot{\mathbf{M}}|^2, \tag{22}$$

where $\mathbf{M}=\mu\Sigma_i\langle\mathbf{s_i}\rangle$ is the total magnetic moment of the system. Using the derivative operator introduced in Eq. (13) the maximum value of SR intensity can be written as a series in powers of gN,

$$I = \gamma N^2 \omega_0^4 (\alpha_1 + \beta_1 (gN)^2 + \cdots), \tag{23}$$

where α_1, β_1, are coefficients which depend on the constants c_1 and c_2, which in turn depend on the initial parameters of the spin system. The results of the numeric simulation described in Sec. V are in good agreement with this prediction when $gN \ll 1$.

When the dominant interaction of the spins is with the resonant circuit rather then the external magnetic field, $gN \gg 1$. In a similar manner to Eq. (13), S^+, S^-, S^z and the derivative operator may be expanded in powers of $1/gN$, rather than gN. In this case, t_0 is not associated with Zeeman oscillations, but with the interaction of the spins and the coil. Under these circumstances the characteristic time for this process is much shorter than that of the Zeeman oscillations. However, the mean-field approach, which forms the basis of any analysis of this type, requires that the time scale for all other processes be significantly longer than that of Zeeman oscillations.[10] Therefore, when $gN \gg 1$, this method cannot be used to describe the behavior of such a system of spins.

The single particle approach is retained in the presence of dipole-dipole interactions by including transverse Bloch damping terms in the equation of motion of the magnetic moment of the system. These equations lead to the solution[12]

$$\rho^2 = \frac{\xi^2}{\cosh^2\left(-\frac{1}{2}\xi t' + \frac{1}{2} \ln \frac{\xi + 2\frac{\Omega}{\tau_2} + \cos\theta(0)}{\xi - 2\frac{\Omega}{\tau_2} - \cos\theta(0)} \right)}, \tag{24}$$

where the function $\rho(t)$ is defined through the relations $\rho \cos\phi = M_x/M_0, \rho \sin\phi = M_y/M_0, n_z = M_z/M_0$, M_0 is the magnitude of M at $t=0$; $n_z = \rho^2/2$.

In Eq. (24),

$$\xi = \sqrt{1 + 4\frac{\Omega}{\tau_2}\cos\theta(0) + 4\frac{\Omega^2}{\tau_2^2}}, \quad \Omega = 1/gN\mathcal{L}, \quad \tau_2 = \omega_0 T_2,$$

where T_2 is transverse relaxation Bloch time. In this case the intensity is given by

$$I = \frac{2}{3c^3}\omega_0^4 M_0^2 \rho^2. \tag{25}$$

This expression is similar in form to the theoretical prediction for the intensity of super-radiation in optical region.[13]

The relative importance of dipole-dipole interactions and interaction with the resonant coil is determined by the magnitude of Ω/τ_2. If dipole-dipole interactions dominate, $\Omega/\tau_2 \gg 1$, and the expression for intensity, Eq. (25), becomes

$$I = \frac{32}{3c^3}\omega_0^4 M_0^2 \sin^2\theta(0) e^{-(2\Omega t'/\tau_2)}. \tag{26}$$

On the other hand, if the interaction with the resonant coil is dominant, $\Omega/\tau_2 \ll 1$. In this case, if the initial deviation angle $\theta(0) > \pi/2$, $I(t)$ has a maximum, the magnitude of which decreases as the field of the resonant coil decreases, equivalent to the effect of increasing temperature. This maximum disappears when $\Omega/\tau_2 \geqslant -\frac{1}{2}\cos\theta(0)$.

When the angular deviation of the single particle magnetic moment from its equilibrium position is small, the behavior of the system may be described via a "linear response" approach[12] instead of including Bloch damping. In this case the resonant line shape is given by,

$$\tilde{g}(\Delta) = \frac{1}{\pi}\int_0^\infty e^{-i\Delta t} G(t) dt, \tag{27}$$

where $G(t)$, the free induction decay function, important in magnetic resonance experiments, is defined through

$$M^+ = M_0 \vartheta e^{-i\omega_0 t} G(t), \tag{28}$$

with $M^+ = M_x + iM_y = \mu \Sigma_i \langle s_i^x + i s_i^y \rangle$. $\tilde{g}(\Delta)$ may be determined from the relationship,

$$\frac{1}{\tilde{g}(\Delta)} = \frac{1}{\tilde{g}_0(\Delta)} + \pi\left(\frac{1}{\tau} - i\delta\right), \tag{29}$$

where δ is a constant whose value depends on the initial parameters of the system, $\tilde{g}_0(\Delta)$ is the resonant line shape function when the resonant circuit is not present and τ is the time delay,

$$\tau = \Omega/\omega_0. \tag{30}$$

It is seen from (30) that $\tau \sim 1/N$. Comparison of this theoretical prediction and the results of our numeric simulation are presented in Sec. V.

IV. NUMERIC SIMULATION

The summations in Eqs. (9) and (10) are limited to the $N-1$ nearest spins. In order to ensure that each spin in our cubic lattice has the same number of neighbors we adhere to the common practice in the modeling of such systems[14] of requiring periodic boundary conditions. For a cube of side L, centered at the origin, with vectors $\mathbf{L}_1$, $\mathbf{L}_2$, and $\mathbf{L}_3$ defined by $\mathbf{L}_1 = (L,0,0)$, $\mathbf{L}_2 = (0,L,0)$, and $\mathbf{L}_3 = (0,0,L)$, the boundary conditions are given by,

$$\mathbf{s}(\mathbf{x}) = \mathbf{s}(\mathbf{x} \pm \mathbf{L}_\alpha), \quad \alpha = 1,2,3,$$

for any point $\mathbf{x}$. The results of the modeling of spin systems over short time periods is known to be insensitive to the number of spins,[16,17] thus reducing the possible effect of requiring periodic boundary conditions.

It is not feasible to diagonalize the quantum Hamiltonian for spin systems of the size being considered in this analysis. However, for such cases, a methodology in which each spin is considered a "classical spin" is commonly applied. Formally, this is equivalent to taking the limits $s \gg 1$ and $\hbar \to 0$ such that $\hbar s$ remains constant. Therefore, following the work of many others, in our numeric simulation we will follow this approach. In this case, the system is described by $3N$ differential equations representing these classical spins [Eqs. (9) and (10) and the conjugate of Eq. (10)]. Numerical simulations for "classical" spin systems have been used by many

authors to investigate topics such as MR line shapes and free induction decay,[15,18] spin diffusion,[16] and spin glasses.[17] In those situations where a quantum phenomenological approach is feasible, such as the method of moments or the truncated dipolar interaction approximation, the results of such quantum methods are qualitatively similar to the classical methodology and both are in agreement with experiment. There is particularly good agreement over the time scales involved in this study. In calculating the central moments, up to M_8, Jensen and Hansen[18] found that the classical spin approximation provides an accurate description of NMR line shapes. In addition, Tang and Waugh[19] showed that the free induction decay process calculated numerically for a system of 729 classical spins is in good agreement with experiment. Our analysis involves a system of nuclear spins occupying every lattice site (maximum possible spin density), identical to the systems studied in the previous two references. The condition for the time evolution of large groups of spins to behave in a similar manner is that the collective radiation wavelength is much larger than the separation of the individual spins, which is always valid for NMR radio-frequency wavelengths.

In classical spin methodology spins are treated as classical vectors, whose initial distribution defines the initial conditions of the differential equations which describe the behavior of the spin system. The initial spin distribution can be defined via the Boltzmann energy distribution,

$$F(\cos\theta) = \frac{\lambda}{2\sinh(\lambda)} e^{(-\lambda\cos\theta)}, \tag{31}$$

where θ is the angle between the direction of spin and the direction of the magnetic field and $\lambda = \mu H / k_b T$ is determined by the desired initial polarization of the system. In our computer simulation we start with the uniformly distributed random quantity $x = \cos\theta$, in which case the function

$$F(x) = \frac{\lambda}{2\sinh(\lambda)} \int_{-1}^{x} e^{(-\lambda x')} dx' = \frac{1}{2\sinh(\lambda)} (e^{\lambda x} - e^{-\lambda}) \tag{32}$$

gives the Boltzmann distribution.

The initial spin distribution can also be assigned by a Monte Carlo technique similar to the procedure of Metropolis *et al.*[20] This technique considers the overall spin polarization of the sample which is related to the temperature through the Langevin formula

$$p = \coth(\lambda) - 1/\lambda. \tag{33}$$

A random configuration of spins $\{\mathbf{s}_i\}_{i=1}^{N}$ is taken as the first member of a Gibbs ensemble of spin arrays and its polarization p_{init}, is evaluated. A new direction is chosen randomly for an arbitrary spin and the new total polarization p', is calculated. If $\Delta p = |p' - p_0|$ is less than $\Delta p_{\text{init}} = |p_{\text{init}} - p_0|$, where p_0 is the desired initial polarization of the system, the array with the changed spin is chosen as the second member of the Gibbs ensemble; if it is not rejected. This procedure is repeated until an array of spins is achieved whose polarization is very close to p_0. The array so obtained is taken as the initial spin distribution of the system. In this analysis we set the maximum possible value of the desired initial polarization p_0, to be unity.

A probability distribution similar to that of the Boltzmann distribution can be obtained using the Metropolis method. We have been unable to find the details of this method published elsewhere. Therefore, we present our technical details in the hope that they may prove useful for others involved in the simulation of spin systems.

After the $(n+1)$th step, the probability that the z component of the jth spin is between y and $y+dy$ is given by

$$dp_j^{n+1}(y) = dp_j^n(y)\left(\frac{N-1}{N} + \frac{1+y}{2N}\right) + \frac{1}{N}\int_{-1}^{y} dp_j^n(y_1)\frac{1-y_1}{2}\frac{dy_1}{1-y_1}. \tag{34}$$

The first term represents the case in which there is no change in the z component since a different spin is selected. The second term describes the case in which the new z component is smaller. The third term describes the case of a larger z component. Introducing the function f,

$$dp_j^n(y) = f_n dy,$$

we may write

$$f_{n+1}(y) = \frac{1}{N}\left(N + \frac{y-1}{2}\right) f_n(y) + \frac{1}{2n}\int_{-1}^{y} dy_1 f_n(y_1). \tag{35}$$

Assuming the number of required steps is very large, n may be considered a continuous variable. With $t = n/N$, Eq. (35) can be written for the function $f(t,y)$,

$$\frac{\partial^2 f}{\partial t \partial y} = \frac{y-1}{2}\frac{\partial f}{\partial y} + f. \tag{36}$$

The boundary conditions on f are

$$f(0,y) = \frac{1}{2}, \quad \frac{\partial f(t,-1)}{\partial t} = f(t,-1), \quad \frac{\partial f(t,1)}{\partial n} = \frac{1}{2},$$

which become

$$f(0,y) = \tfrac{1}{2}, \quad f(t,-1) = \tfrac{1}{2}e^{-t}, \quad f(t,1) = \tfrac{1}{2}(1+t). \tag{37}$$

Performing a Laplace transformation of function f over variable t gives

$$s\frac{\partial f(s,y)}{\partial y} = \frac{y-1}{2}\frac{\partial f(s,y)}{\partial y} + f(s,y), \tag{38}$$

the solution of which is

$$f(s,y) = \frac{c(s)}{(y-1-2s)^2}. \tag{39}$$

Applying the boundary conditions (37), followed by the inverse transformation, gives

$$f(t,y) = \frac{1}{2} e^{(t/2)(y-1)}\left(1 + \frac{t}{2}(1+y)\right), \tag{40}$$

the probability distribution for the Metropolis method.

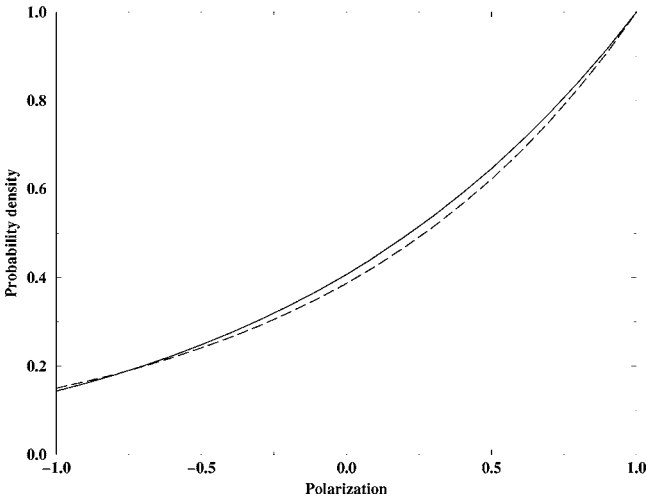

FIG. 1. Normalized z component of spin polarization versus probability distribution for the two methods of obtaining the initial spin distribution. Solid line, Metropolis method; dashed line, Boltzmann method.

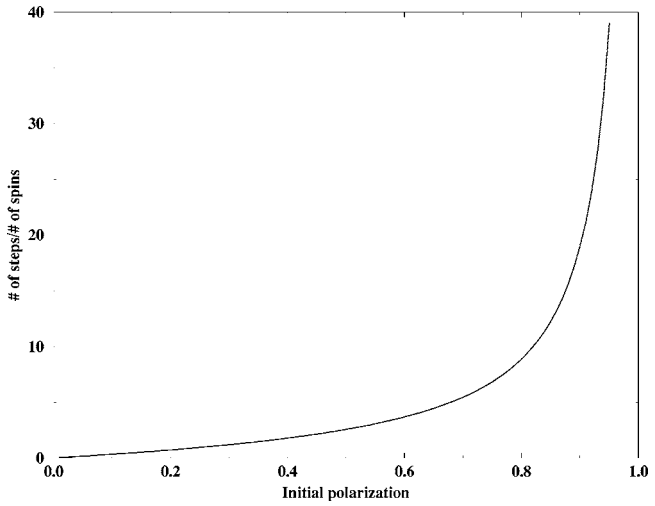

FIG. 2. Desired polarization versus the ratio of the number of steps to the number of spins, for the Metropolis method of obtaining an initial spin distribution.

The probability distributions for the Boltzmann and Metropolis methods are compared in Fig. 1. In this figure the probability distributions for both methods are plotted versus the (normalized) z component of a particular spin when the initial polarization is 30%. An initial polarization of approximately this value leads to the largest discrepancy between the two probability distributions. Nevertheless, even in this case, the distributions are similar enough that we can be confident that either method will lead to an appropriate initial spin distribution.

Using the Metropolis method the polarization of the system is defined by

$$p = \int_{-1}^{1} yf(t,y)dy = \frac{(2 + t^2 - 2t - 2e^{-t})}{t^2}. \tag{41}$$

For a given polarization, (41) allows us to determine the parameter t and therefore the number of steps needed to reach the desired initial distribution of spins. In Fig. 2 the parameter t, the ratio of the number of required steps to the number of spins in the system, is plotted versus the required polarization. For the Boltzmann method the number of steps is exactly equal to the number of spins in the system. Therefore, from Fig. 2 it is clear that for an initial spin distribution requiring a large polarization the Boltzmann method will require significantly fewer steps. For this reason we use the Boltzmann method to determine initial spin distributions in our numeric simulation.

The time evolution of any spin system clearly depends on the initial configuration of the spins, but there are many different initial spin configurations which correspond to a specific initial polarization of the system. Therefore, in order to describe the time evolution of a system of particular polarization, it is appropriate to obtain a thermodynamic average over the canonical ensemble of initial spin configurations having the same initial polarization. Each member of the ensemble is a solution of Eqs. (9) and (10), completely independent of any other solution. This independence means that thermodynamic averaging can most efficiently be achieved by allowing each processor in a multiprocessor architecture to determine the numeric solution of a different initial configuration in parallel. In the next section the results of our numeric simulation are compared with theoretical predictions. The numeric simulation curves in the figures describing the time evolution of various parameters of the spin system all represent an average over 500 initial spin distributions obtained using a multiprocessor parallel architecture described above. Each initial spin distribution is created via the Boltzmann method described above.

V. COMPARISON OF NUMERIC SIMULATION AND THEORETICAL PREDICTIONS

The role of dipole-dipole interactions in determining the behavior of a system of spins has been investigated by applying our numerical simulation to a system of 1331 spins $(11 \times 11 \times 11)$, including and excluding dipole-dipole interactions. In Sec. III, the characteristic time for the polarization of the system to reach zero, given by Eq. (30), which also characterizes the time taken to reach maximum SR intensity, is seen to depend on three parameters: the external field ω_0, the coupling constant g, and number of spins in the system N. With the number of spins in the system fixed, we can alter this characteristic time by adjusting the values of ω_0 and g in our simulation. Figures 3(a)–3(d) display the time evolution of the normalized SR intensity for four different values of this characteristic time. In each figure there are two curves representing the spin system with and without dipole-dipole interactions. In the units employed in this simulation the characteristic time for dipole-dipole interactions is of order unity. It is clear from the figures that as the time taken for the SR intensity to reach its maximum value increases, the disparity between the curves including and excluding dipole-dipole interactions also increases. Therefore, as expected,

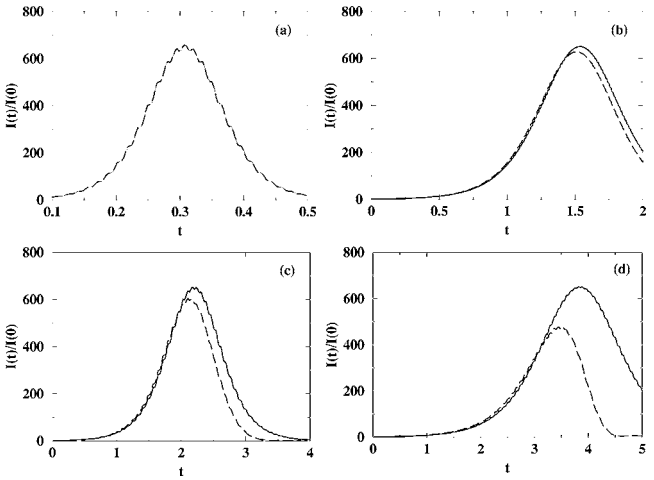

FIG. 3. Numeric simulation results of SR intensity ration $I(t)/I(0)$ as a function of dimensionless time for different values of the spin inversion time. Solid line, dipole-dipole interactions neglected; dashed line, dipole-dipole interactions included. Four different spin inversion times are displayed, corresponding to different pairs of values of g and ω_0. Initial polarization is 0.475(95%) in all cases. (a) $g=0.0001$, $\omega_0=200$; (b) $g=0.00002$, $\omega_0=200$; (c) $g=0.00007$, $\omega_0=40$; (d) $g=0.00004$, $\omega_0=40$.

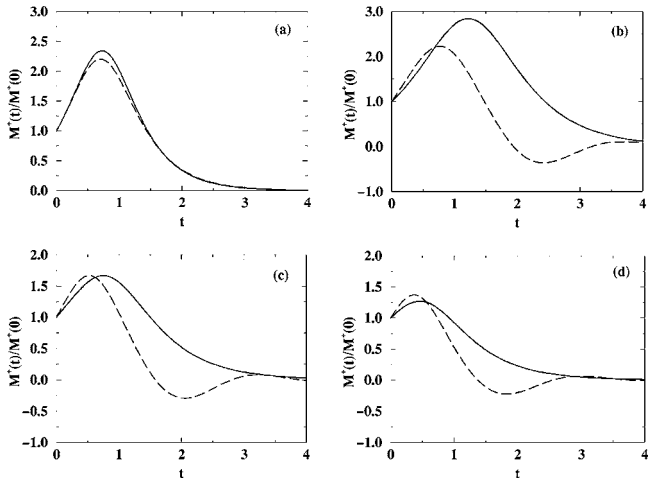

FIG. 4. $M^+(t)/M^+(0)$ as a function of dimensionless time. Solid line, Bloch relaxation theoretical prediction; dashed line, numeric simulation. (a) Dipole-dipole interactions neglected; $\omega_0=200$, initial polarization=0.3, initial angle between magnetic moment and the external field $\theta(0)=2.7$ radians (155°): (b)–(d) Dipole-dipole interactions included, $\omega_0=200$, initial polarization 0.3; (b) $\theta(0)=2.9$ radians (166°); (c) $\theta(0)=2.7$ radians (155°); (d) $\theta(0)=2.5$ radians (143°).

when the time taken for the SR intensity to reach its maximum value, or equivalently the time taken for the polarization of the system to reach zero, is comparable or shorter than the characteristic time for dipole-dipole interactions, dipole-dipole interactions do not play a significant role and can be neglected in numeric simulations.

In Sec. III, the Bloch relaxation method was used to obtain an expression for $\rho(t)$, (24), as a function of the initial angle $\theta(0)$, between the magnetic moment $\mathbf{M}$ and the direction of the external field H_0. Note that $\rho(t)$ is proportional to $M^+(t)$, where $M^+=\mu\Sigma_i\langle s_i^x+is_i^y\rangle$. In the numeric simulation $M^+(t)$ at arbitrary $\theta(0)$ is obtained by solving Eqs. (9) and (10) in the coordinate system which rotates about the magnetic field with the spin precession frequency. In this system, if an additional coil is placed orthogonal to the original coil, cylindrical symmetry is achieved, eliminating the ω_0 dependent terms in (9) and (10). With these terms eliminated, the time dependence of $M^+(t)$ can be found from the numeric simulation using an integration step size ω_0 times larger without compromising accuracy and stability. The only significant effect of including an additional coil is a factor of 2 increase of the interaction with the spin system, such that the dimensionless parameter Ω is redefined as $\Omega=1/2gNM_0$. Since Bloch relaxation methodology is most reliable at high spin temperature, the numeric simulation and theoretical prediction are compared at a Boltzmann factor $\mu H/k_bT$, of approximately unity, corresponding to an initial polarization of 0.3 (60%). A system of 343 ($7\times7\times7$) spins is simulated with the coupling constant $g=0.0001$; the value of g chosen to be large enough to ensure spin inversion when $\theta(0)\sim\pi$, but not so large that there is no difference between neglecting and including dipole-dipole interactions.

Figure 4(a) compares the time dependence of $M^+(t)/M^+(0)$ using the Bloch relaxation method with the result of the numeric simulation for $\theta(0)=2.7$ radians (155°), under conditions when dipole-dipole interactions can be neglected. $M^+(t)$ from the Bloch relaxation method is obtained through $\rho(t)$ from Eq. (24) by allowing the Bloch relaxation time T_2, to become very large. The numeric simulation curve represents an average over 500 different initial spin configurations, each with the same initial polarization of 0.3. As indicated in the previous section, a multiprocessor computing architecture allowed us to consider such a large number of initial spin configurations. It can be seen from the figure there is good agreement between the theoretical prediction and the numeric simulation. The two curves reach their maxima at almost exactly the same time, although there is a slight difference in the magnitude of the maxima.

Figures 4(b)–4(d) compare the time dependence of $M^+(t)/M^+(0)$ using the Bloch relaxation method with the result of the numeric simulation when dipole-dipole interactions are included. Under these conditions the Bloch relaxation time T_2, is of order unity. For each value of $\theta(0)$ there is a corresponding specific value of T_2 which produces the best agreement between the theoretical prediction and the numeric simulation. The curves shown in Figs. 4(b)–4(d) represent three different values of $\theta(0)$; in each case the theoretical curve is calculated with $T_2=1.45$, the value of T_2 which gives the best overall agreement. As in the case when dipole-dipole interactions are ignored, each numeric simulation curve represents an average over 500 different initial spin configurations having the same initial polarization of 0.3. When comparing the theoretical and numeric simulation curves it is important to realize that Bloch relaxation theory cannot reproduce the secondary maxima generated by the numeric simulation. Therefore, a meaningful comparison should be limited to the location (in time) and magnitude of the first peak in $M^+(t)/M^+(0)$. Nevertheless, these figures

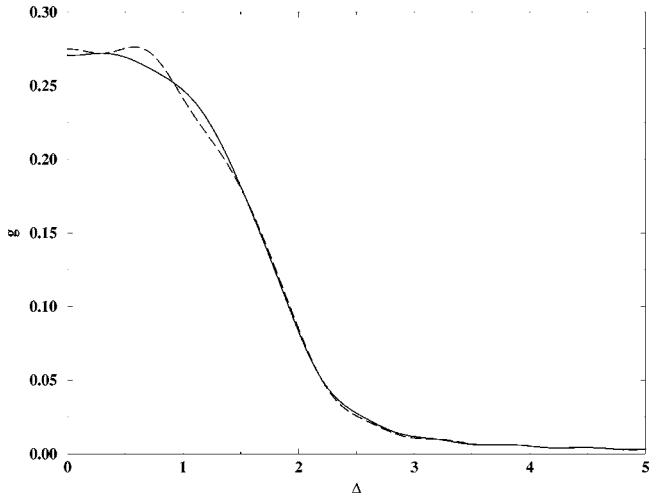

FIG. 5. $g(\Delta)$ as a function of Δ. Solid line, linear response theoretical prediction; dashed line, numeric simulation.

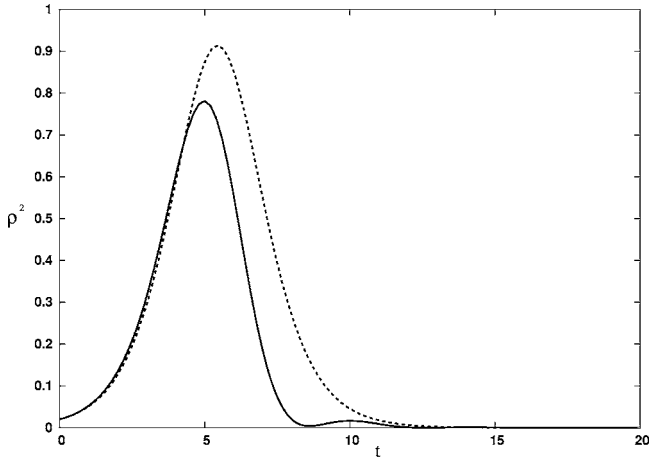

FIG. 7. ρ^2 as a function of dimensionless time. Same values of the parameters as in Fig. 6. Solid line, numeric simulation; dashed line, Bloch solution (24).

show that Bloch relaxation provides a qualitative description of this non-equilibrium system.

In Sec. III the linear response method is described, by which the resonant line shape $\tilde{g}(\Delta)$ may be obtained when the single particle magnetic moment deviates by a small angle from its equilibrium position. Figure 5 compares the numeric simulation of $\tilde{g}(\Delta)$ with the linear response prediction from Eq. (29). The $\tilde{g}_0(\Delta)$ in (29) is obtained from the numeric simulation without including the resonant coils. The two curves in Fig. 5 are in good agreement demonstrating the consistency of our numeric simulation.

Another peculiarity of SR phenomena is the presence of secondary maxima in the amplitude of the transverse magnetization $\rho=\sqrt{(M_x^2+M_y^2)}/M_0$, Fig. 6. The quantity ρ^2 is proportional to the radiation intensity,[12] which also exhibits secondary maxima, Fig. 7. It is seen that secondary maxima are easier to observe in the transverse magnetization ρ. Note that the maximum in ρ for large t corresponds to the maximum in the Fourier transform of the free induction decay function, $\tilde{g}(\Delta)$, commonly used in magnetic resonance applications. A hint of the secondary maximum is seen in Fig. 5 for $g(\Delta)=\mathrm{Re}\,\tilde{g}(\Delta)$ at small $\Delta=\omega-\omega_0$ (Δ measures the departure from resonance). All these maxima disappear if the initial deviation of the magnetic moment from its equilibrium position along the z axis, $\theta(0)$, is far from π (in Figs. 6 and 7 the value of this angle is 172°). To our knowledge, the phenomenon of secondary maxima, both in transverse magnetization and radiation intensity has not previously been reported. There is no analogy between this effect and spin-echo since our situation does not involve external pulses.

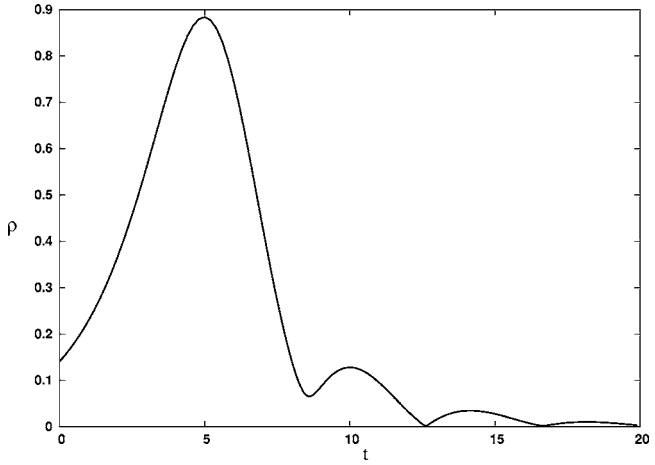

FIG. 6. Numeric simulation of ρ as as function of dimensionless (in units of T_d) time. Initial polarization is 0.475 (95%), $\omega_0=200$, $g=0.0001$, $N=343$.

As well as the numeric simulation, Fig. 7 shows the quantity ρ^2 for the Bloch solution, in which $\rho\propto 1/\cosh((t-t_0)/\tau)$. It can be seen that the Bloch solution describes qualitatively the shape of the radiation intensity and is in good quantitative agreement with the numeric simulation during the initial stage of the process. However, at later stages, when dipole interactions are important (they are less significant when the radiation peak occurs at very short times, $t\ll T_2$), it is not adequate even in the region of the primary maximum and, of course, it does not exhibit secondary maximum.

VI. CONCLUSION

We have investigated several aspects of the coherent behavior of a system of polarized spins where magnetic dipole radiation is emitted in the radio-frequency region. The radiation intensity is proportional to N^2, the characteristic SR time $\tau=\Omega/\omega_0\sim 1/N$. The peak of the intensity is sharper the shorter the delay time and its width increases as the delay time increases (compared to T_d).

The Bloch relaxation method has been used to describe a spin system when dipole-dipole interactions are included. In this case, the time evolution of the magnetic moment of the system can be determined as a function of the initial angle between the magnetic moment and the external magnetic field. Qualitative agreement between this prediction and our numeric simulation, based on the microscopic Hamiltonian,

is observed. Results of the linear response method, appropriate when the single particle magnetic moment deviates by a small angle from its equilibrium position, are also seen to be in good agreement with the numeric simulation.

As part of our numeric simulation we considered two methods of obtaining an initial spin distribution for a specific desired system polarization. Both the Metropolis and Boltzmann methods produce acceptable initial spin distributions. However, the Boltzmann method is favored, since in the Metropolis method the number of steps required to produce a desired polarization increases rapidly as the polarization approaches unity. Thermodynamic averaging over multiple initial spin distributions, each having the same initial polarization, is achieved in a multiprocessor environment.

The role of dipole-dipole interactions for SR phenomena is studied in detail. Simple models for these interactions and a phenomenological approach based on the Bloch equations qualitatively describe some aspects of SR relaxation. These models, together with numeric simulations based on a microscopic consideration of dipole-dipole interactions allow us to obtain a reliable description of spin system radio-frequency SR. Secondary peaks in observable quantities associated with SR relaxation have been observed. These peaks are specific for SR from highly polarized and almost completely inverted spin systems. They do not appear in the phenomenological approach, but are observed if dipole-dipole interactions are taken into account microscopically, through the dipole-dipole interaction Hamiltonian.

[1] L. Allen and J. Eberly, *Optical Resonance and Two-Level Atoms* (Wiley, New York, 1975); A. V. Andreev, V. I. Emelyanov, and Y. A. Ilinski, *Cooperative Effects in Optics* (Institute of Physics, Bristol, 1993); M. E. Crenshaw, M. Scalora, and C. M. Bowden, Phys. Rev. Lett. **68**, 911 (1992); J. Rai and C. M. Bowden, Phys. Rev. A **46**, 1522 (1992).

[2] A. Abragam and M. Goldman, *Nuclear Magnetism, Order and Disorder* (Clarendon, Oxford, 1982).

[3] T. S. Belozerova, V. K. Henner, and V. I. Yukalov, Phys. Rev. B **46**, 682 (1992).

[4] T. S. Belozerova, V. K. Henner, and V. I. Yukalov, Comput. Phys. Commun. **73**, 151 (1992).

[5] N. Bloembergen and R. V. Pound, Phys. Rev. **95**, 8 (1954).

[6] P. Bosiger, E. Brun, and D. Meier, Phys. Rev. Lett. **38**, 602 (1977).

[7] Y. F. Kiselev, A. F. Prutkoglyad, A. S. Shumovsky, and V. I. Yukalov, Sov. Phys. JETP **38**, 602 (1977).

[8] V. I. Yukalov, Phys. Rev. B **53**, 9232 (1996); V. I. Yukalov and E. P. Yukalova, Laser Phys. **11**, 546 (2001).

[9] T. S. Belozerova, C. L. Davis, and V. K. Henner, Phys. Rev. B **58**, 3111 (1998).

[10] E. K. Henner, Solid State Phys. **26**, 2779 (1984).

[11] M. Goldman, *Spin Temperature and Nuclear Magnetic Resonance in Solids* (Pergamon, Oxford, 1970).

[12] C. L. Davis, I. V. Kaganov, and V. K. Henner, Phys. Rev. B **62**, 12328 (2000).

[13] V. V. Andreev, V. I. Emel'yanov, and Yu. A. Il'inskiĭ, Usp. Fiz. Nauk **131**, 653 (1980) [Sov. Phys. Usp. **23**, 493 (1980)].

[14] *Monte Carlo Methods in Statistical Physics*, edited by K. Binder (Springer-Verlag, Berlin, 1979).

[15] S. Jensen and O. Platz, Phys. Rev. B **7**, 31 (1973).

[16] D. K. Sodickson and J. S. Waugh, Phys. Rev. B **52**, 6467 (1995).

[17] S. L. Ginzburg, *Irreversible Phenomena in Spin Glasses* (Nauka, Moscow, 1989).

[18] S. Jensen and E. Hansen, Phys. Rev. B **7**, 2910 (1973).

[19] C. Tang and J. S. Waugh, Phys. Rev. B **45**, 748 (1992).

[20] N. Metropolis *et al.*, J. Chem. Phys. **21**, 1087 (1953).